Appl. Math. Mech. -Engl. Ed., **36**(12), 1555–1568 (2015)
DOI 10.1007/s10483-015-2005-6

Applied Mathematics and Mechanics (English Edition)

Sensitivity analysis of pull-in voltage for RF MEMS switch based on modified couple stress theory*

Junhua ZHU[1,2†], Renhuai LIU[1,2,3]

1. Science and Technology on Reliability Physics and Application Technology of Electronic Component Laboratory, Guangzhou 510610, China;
2. China Electronic Product Reliability and Environmental Testing Research Institute, Guangzhou 510610, China;
3. Institute of Applied Mechanics, Jinan University, Guangzhou 510632, China

Abstract An approximate analytical model for calculating the pull-in voltage of a stepped cantilever-type radio frequency (RF) micro electro-mechanical system (MEMS) switch is developed based on the Euler-Bernoulli beam and a modified couple stress theory, and is validated by comparison with the finite element results. The sensitivity functions of the pull-in voltage to the designed parameters are derived based on the proposed model. The sensitivity investigation shows that the pull-in voltage sensitivities increase/decrease nonlinearly with the increases in the designed parameters. For the stepped cantilever beam, there exists a nonzero optimal dimensionless length ratio, where the pull-in voltage is insensitive. The optimal value of the dimensionless length ratio only depends on the dimensionless width ratio, and can be obtained by solving a nonlinear equation. The determination of the designed parameters is discussed, and some recommendations are made for the RF MEMS switch optimization.

Key words stepped cantilever beam, pull-in voltage, modified couple stress theory, radio frequency (RF) micro electro-mechanical system (MEMS) switch, analytical solution, sensitivity analysis

Chinese Library Classification TN701, TN401
2010 Mathematics Subject Classification 74M25, 74A60

1 Introduction

The electrostatic actuation is the most popular actuation used in micro/nano electromechanical systems (MEMSs/NEMSs) due to its many inherent advantages. Various electrostatic actuators have been developed and utilized in a wide variety of applications, including micro/nano motors, micro/nano switches, micro/nano relays, micro/nano resonators, micro mirrors, micro pumps, micro valves, and micro/nano filters[1]. For electrostatic MEMS/NEMS devices, pull-in is a basic phenomenon, and its instability is fundamental to the design and optimization of the MEMS/NEMS devices.

* Received Dec. 31, 2014 / Revised Jun. 12, 2015
Project supported by the National Natural Science Foundation of China (Nos. 51505089 and 61204116), the Opening Project of the Science and Technology on Reliability Physics and Application Technology of Electronic Component Laboratory (Nos. ZHD201207 and 9140C030605140C03015), and the Pearl River S&T Nova Program of Guangzhou (No. 2014J2200086)
† Corresponding author, E-mail: zhujh@ceprei.com

Although the pull-in instability is amongst the most studied MEMS/NEMS phenomena, the involved mechanisms are still not fully understood[1–3], especially for variable cross-section microstructural devices. In the past few years, many pull-in voltage prediction models have been proposed for the micro-structures widely used in MEMS devices, e.g., cantilever beams[4–8] and double clamped beams[4,9–10]. Some of these models have also considered the size effects occurring on the micro/nano scale, e.g., models based on the modified couple stress theory[4] and the nonlocal elasticity theory[11]. However, most of them focus on either the constant cross-section micro/nano beams[4–6,9–11] or the methods for solving the partial differential equations[4,6,10]. In fact, many MEMS devices have to be designed with the variable cross-section micro/nano beams so as to obtain the intended pull-in voltage[12–13]. For these variable cross-section microstructures, a lot of time must be spent in modeling the devices and computing the numerical solutions of the pull-in voltage with the help of the commercial softwares such as ANSYS and COVENTOR. Even so, most of the commercial softwares are developed based on the classical continuous theory, which cannot give the size-dependent solutions, and even cannot display the relationship between the pull-in voltage and the structural parameters explicitly.

In this paper, an approximate analytical solution of the pull-in voltage prediction for a stepped cantilever-type radio frequency (RF) MEMS switch is proposed based on the Euler-Bernoulli beam theory and a modified couple stress theory, and is validated by a comparison with the finite element solutions. The sensitivities of the pull-in voltage to the designed parameters, including the material, structural, and dimensionless parameters, are derived analytically based on the proposed model. Some new characteristics of the stepped cantilever beam are observed, and some conclusions are made for the RF MEMS switch optimization.

2 Mathematical modeling

2.1 Pull-in voltage prediction model

A stepped cantilever-type RF MEMS switch is shown in Fig. 1, which consists of a movable electrode and a fixed electrode. The movable electrode has two cantilever bars with the length L_1, the width b_1, and the thickness h. The gap between each cantilever bar is d. The two cantilever bars are connected by an anchor. The supported cantilever bars are then connected with a beam of the length L_2, the width b_2, and the thickness h. The total length of the cantilever-type RF MEMS switch is L, i.e.,

$$L = L_1 + L_2.$$

The fixed electrode with the width b_2 and the length L_2 is located at the position L_1. The initial gap height between the movable and the fixed electrodes is g_0. Based on the assumption of the Euler-Bernoulli beam and a modified couple stress theory, the total mechanical bending strain energy U_{m} can be expressed as the sum of those of the two cantilever bars ($L_1 \times b_1 \times h$) and the beam ($L_2 \times b_2 \times h$)[4,6,14], i.e.,

$$U_{\mathrm{m}} = \int_0^{L_1} (EI_1 + \mu A_1 l^2) w''^2 \mathrm{d}x + \frac{1}{2} \int_{L_1}^{L} (EI_2 + \mu A_2 l^2) w''^2 \mathrm{d}x, \tag{1}$$

where E and μ are the effective Young's modulus and the shear modulus, respectively, and l represents the material length scale parameter, which is a scale parameter that reflects the impurities or defects of the material on micro/nano scale. The material length scale parameter must be experimentally determined for each material, e.g., for the silicon $\langle 110 \rangle$ and polysilicon, and the parameter l has an order of magnitude of 10^{-1} μm[4]. I_1 and I_2 represent the cross-sectional area moments of the inertia defined by

$$I_1 = \frac{1}{12} b_1 h^3, \quad I_2 = \frac{1}{12} b_2 h^3.$$

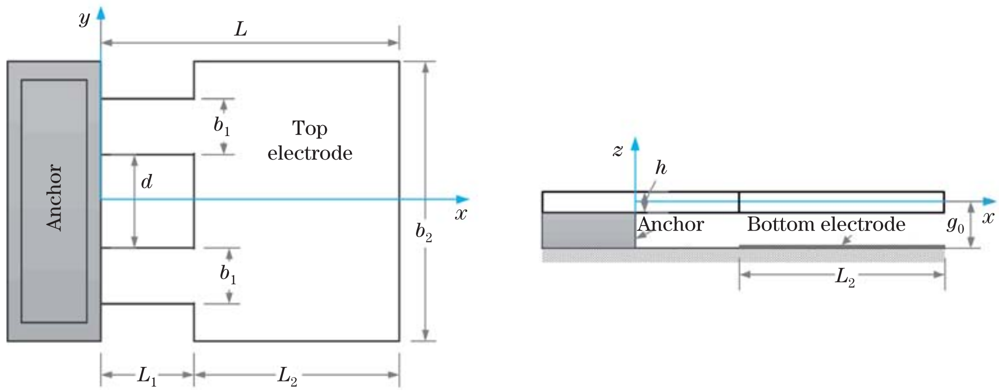

(a) Top view (b) Side view

Fig. 1 Top and side view of stepped cantilever-type RF MEMS switch

A_1 and A_2 represent the cross-sectional areas defined by

$$A_1 = b_1 h, \quad A_2 = b_2 h.$$

w'' is the second-order derivative of the deflection w with respect to the position x.

Introduce the following dimensionless parameters[15]:

$$\alpha = \frac{L_1}{L}, \quad \beta = \frac{b_1}{b_2}, \quad X = \frac{x}{L}, \quad W = \frac{w}{g_0}, \tag{2}$$

where α is the dimensionless length ratio, $0 \leqslant \alpha < 1$, and the larger the dimensionless length ratio is, the smaller the distribution region size is. β is the dimensionless width ratio, $0 < \beta \leqslant 0.5$. When $\beta = 0.5$, the cantilever beam becomes a constant cross-section cantilever beam. W is the dimensionless beam deflection function, and $0 \leqslant W \leqslant 1$, reflecting the electrostatic force distribution region size along the axial direction. Then, substituting Eq. (2) into Eq. (1) yields the equation in the dimensionless form as follows:

$$U_{\mathrm{m}} = \frac{\kappa E b_2 h^3 g_0^2}{12L^3}\Big(\beta\int_0^{\alpha} W''^2 \mathrm{d}X + \frac{1}{2}\int_{\alpha}^{1} W''^2 \mathrm{d}X\Big), \tag{3}$$

where κ is the size dependent coefficient defined by

$$\kappa = 1 + \frac{6l^2}{(1+\nu)h^2}.$$

Assuming that W is defined by[4, 15]

$$W(X) = \eta\varphi(X), \tag{4}$$

where η is the associated modal participation factor, $\varphi(X)$ is the first natural mode of the cantilever beam per unite length defined by

$$\varphi(X) = (\cosh(\lambda X) - \cos(\lambda X)) - \gamma(\sinh(\lambda X) - \sin(\lambda X)).$$

In the above equation,

$$\begin{cases} 0 \leqslant X \leqslant 1, \quad \lambda = 1.875\,104\,07, \\ \gamma = \dfrac{\cos\lambda + \cosh\lambda}{\sin\lambda + \sinh\lambda} = 0.734\,095\,5. \end{cases}$$

Substituting Eq. (4) into Eq. (3) yields

$$U_{\mathrm{m}}=\frac{\kappa E b_2 h^3 g_0^2}{12L^3}\eta^2\Big(\beta\int_0^{\alpha}\varphi''^2(X)\mathrm{d}X+\frac{1}{2}\int_{\alpha}^{1}\varphi''^2(X)\mathrm{d}X\Big). \tag{5}$$

The total electrical potential energy U_{e} is given by

$$U_{\mathrm{e}}=-\frac{1}{2}V^2\int_{L_1}^{L}\mathrm{d}C, \tag{6}$$

where V is the applied bias voltage, and $\mathrm{d}C$ is the parallel-plate capacitance per unit length between the movable electrode and the fixed electrode defined by

$$\mathrm{d}C=\varepsilon_0\varepsilon_{\mathrm{r}}\frac{b_2}{g_0-w},$$

in which ε_0 and ε_{r} are the permittivities of the free space and the dielectric constant of the dielectric medium between the movable and fixed electrodes, respectively.

Substituting Eqs. (2) and (4) into Eq. (6) yields

$$U_{\mathrm{e}}=-\frac{\varepsilon_0\varepsilon_{\mathrm{r}} b_2 L V^2}{2g_0}\int_{\alpha}^{1}\frac{1}{1-\eta\varphi(X)}\mathrm{d}X. \tag{7}$$

Then, the total potential energy is the sum of the mechanical energy and the electrical potential energy. Employing the principle of the minimum total potential energy for the static deflection of the movable electrode, we can obtain that the first-order variation of the total potential energy is zero at the equilibrium position, i.e.,

$$\delta U=\delta U_{\mathrm{m}}+\delta U_{\mathrm{e}}=b_2(2\eta K-\varepsilon_0\varepsilon_{\mathrm{r}}V^2P(\eta,\alpha))\delta\eta=0. \tag{8}$$

At the transition from a stable to an unstable equilibrium state, the second-order variation of the total potential energy equals zero[16], i.e.,

$$\delta^2 U=\delta^2 U_{\mathrm{m}}+\delta^2 U_{\mathrm{e}}=b_2(2K-\varepsilon_0\varepsilon_{\mathrm{r}}V^2Q(\eta,\alpha))\delta^2\eta=0, \tag{9}$$

where

$$K=\frac{\kappa E h^3 g_0^3(2\beta\zeta_1+\zeta_2)}{12L^4}, \tag{10}$$

$$P(\eta,\alpha)=\int_{\alpha}^{1}F_1(\eta,X)\mathrm{d}X, \tag{11}$$

$$Q(\eta,\alpha)=\int_{\alpha}^{1}F_2(\eta,X)\mathrm{d}X, \tag{12}$$

$$\zeta_1=\int_0^{\alpha}\varphi''^2(X)\mathrm{d}X,\quad \zeta_2=\int_{\alpha}^{1}\varphi''^2(X)\mathrm{d}X, \tag{13}$$

$$F_1(\eta,X)=\frac{\varphi(X)}{(1-\eta\varphi(X))^2}, \tag{14}$$

$$F_2(\eta,X)=\frac{2\varphi^2(X)}{(1-\eta\varphi(X))^3}. \tag{15}$$

From Eqs. (8) and (9), the following two equations can be obtained in order to have the nontrivial solution:

$$2\eta K - \varepsilon_0\varepsilon_{\mathrm{r}}V^2P(\eta,\alpha) = 0, \tag{16}$$

$$2K - \varepsilon_0\varepsilon_{\mathrm{r}}V^2Q(\eta,\alpha) = 0. \tag{17}$$

The above two equations lead to

$$\eta Q(\eta,\alpha) = P(\eta,\alpha). \tag{18}$$

Solving Eq. (18) by the numerical analysis methods, e.g., the simple iteration method, can determine the coefficient η_{p} at the pull-in. Then, substituting η_{p} back into Eq. (17) yields the approximate analytical solution to the pull-in voltage as follows:

$$V_{\mathrm{p}} = \sqrt{\frac{2K}{\varepsilon_0\varepsilon_{\mathrm{r}}Q(\eta_{\mathrm{p}},\alpha)}}. \tag{19}$$

When the beam thickness h is far more than the material length scale parameter l, the size dependent coefficient tends to one, which means that the size effect is negligible. Thus, the pull-in voltage model based on the modified couple stress theory can be reduced to that based on the classical beam theory by setting $\kappa = 1$.

2.2 Sensitivity of pull-in voltage

In order to investigate the effect of various designing parameters on the pull-in voltage, a sensitivity analysis is conducted. The pull-in voltage sensitivities are measured by the partial differential equations of the pull-in voltage with respect to the studied parameters. The sensitivities to the material parameters can be obtained by

$$\begin{aligned}\frac{\partial V_{\mathrm{p}}}{\partial E} &= \frac{1}{\varepsilon_0\varepsilon_{\mathrm{r}}Q(\eta_{\mathrm{p}},\alpha)V_{\mathrm{p}}}\frac{\partial K}{\partial E}\\ &= \frac{\kappa h^3 g_0^3(2\beta\zeta_1+\zeta_2)}{12\varepsilon_0\varepsilon_{\mathrm{r}}L^4Q(\eta_{\mathrm{p}},\alpha)V_{\mathrm{p}}},\end{aligned} \tag{20}$$

$$\frac{\partial V_{\mathrm{p}}}{\partial l} = \frac{2\mu h g_0^3 l(2\beta\zeta_1+\zeta_2)}{\varepsilon_0\varepsilon_{\mathrm{r}}L^4Q(\eta_{\mathrm{p}},\alpha)V_{\mathrm{p}}}. \tag{21}$$

The sensitivities to the dimensionless parameters α and β can be obtained by

$$\frac{\partial V_{\mathrm{p}}}{\partial \alpha} = \frac{1}{\varepsilon_0\varepsilon_{\mathrm{r}}Q^2(\eta_{\mathrm{p}},\alpha)V_{\mathrm{p}}}\Big(Q(\eta_{\mathrm{p}},\alpha)\frac{\partial K}{\partial \alpha} - K\frac{\partial Q(\eta_{\mathrm{p}},\alpha)}{\partial \alpha}\Big), \tag{22}$$

$$\frac{\partial V_{\mathrm{p}}}{\partial \beta} = \frac{1}{\varepsilon_0\varepsilon_{\mathrm{r}}Q(\eta_{\mathrm{p}},\alpha)V_{\mathrm{p}}}\frac{\partial K}{\partial \beta}, \tag{23}$$

where

$$\frac{\partial K}{\partial \alpha} = \frac{\kappa E h^3 g_0^3}{12L^4}\Big(2\beta\frac{\partial \zeta_1}{\partial \alpha} + \frac{\partial \zeta_2}{\partial \alpha}\Big), \tag{24}$$

$$\frac{\partial K}{\partial \beta} = \frac{\kappa E h^3 g_0^3\zeta_1}{6L^4}. \tag{25}$$

According to Leibnitz's rules, we can derive the derivatives of the integrals as follows[17]:

$$\frac{\partial \zeta_1}{\partial \alpha} = \varphi''^2(\alpha), \quad \frac{\partial \zeta_2}{\partial \alpha} = -\varphi''^2(\alpha), \tag{26}$$

$$\frac{\partial Q(\eta_\mathrm{p}, \alpha)}{\partial \alpha} = R(\eta_\mathrm{p}, \alpha)\frac{\partial \eta_\mathrm{p}}{\partial \alpha} - F_2(\eta_\mathrm{p}, \alpha), \tag{27}$$

where

$$R(\eta_\mathrm{p}, \alpha) = 6\int_\alpha^1 \frac{\varphi^3(X)}{(1-\eta_\mathrm{p}\varphi(X))^4}\mathrm{d}X.$$

Calculating the derivative with respect to α on both sides of Eq. (18) yields

$$\frac{\partial \eta_\mathrm{p}}{\partial \alpha}Q(\eta_\mathrm{p}, \alpha) + \eta_\mathrm{p}\frac{\partial Q(\eta_\mathrm{p}, \alpha)}{\partial \alpha} = \frac{\partial P(\eta_\mathrm{p}, \alpha)}{\partial \alpha}. \tag{28}$$

The derivative of the integral function $P(\eta_\mathrm{p}, \alpha)$ is[17]

$$\frac{\partial P(\eta_\mathrm{p}, \alpha)}{\partial \alpha} = Q(\eta_\mathrm{p}, \alpha)\frac{\partial \eta_\mathrm{p}}{\partial \alpha} - F_1(\eta_\mathrm{p}, \alpha). \tag{29}$$

From Eqs. (27)–(29), we have

$$\frac{\partial \eta_\mathrm{p}}{\partial \alpha} = \frac{F_2(\eta_\mathrm{p}, \alpha)}{R(\eta_\mathrm{p}, \alpha)} - \frac{F_1(\eta_\mathrm{p}, \alpha)}{\eta_\mathrm{p}R(\eta_\mathrm{p}, \alpha)}. \tag{30}$$

Substituting Eq. (30) into Eq. (27) yields

$$\frac{\partial Q(\eta_\mathrm{p}, \alpha)}{\partial \alpha} = -\frac{F_1(\eta_\mathrm{p}, \alpha)}{\eta_\mathrm{p}}. \tag{31}$$

The sensitivities to the structural parameters can be obtained by

$$\frac{\partial V_\mathrm{p}}{\partial L_1} = \frac{1}{\varepsilon_0\varepsilon_\mathrm{r}Q^2(\eta_\mathrm{p}, \alpha)V_\mathrm{p}}\Big(Q(\eta_\mathrm{p}, \alpha)\frac{\partial K}{\partial L_1} - K\frac{\partial Q(\eta_\mathrm{p}, \alpha)}{\partial L_1}\Big), \tag{32}$$

$$\frac{\partial V_\mathrm{p}}{\partial L_2} = \frac{1}{\varepsilon_0\varepsilon_\mathrm{r}Q^2(\eta_\mathrm{p}, \alpha)V_\mathrm{p}}\Big(Q(\eta_\mathrm{p}, \alpha)\frac{\partial K}{\partial L_2} - K\frac{\partial Q(\eta_\mathrm{p}, \alpha)}{\partial L_2}\Big), \tag{33}$$

$$\frac{\partial V_\mathrm{p}}{\partial b_1} = \frac{\partial V_\mathrm{p}}{\partial \beta}\frac{\partial \beta}{\partial b_1} = \frac{1}{b_2}\frac{\partial V_\mathrm{p}}{\partial \beta}, \tag{34}$$

$$\frac{\partial V_\mathrm{p}}{\partial b_2} = \frac{\partial V_\mathrm{p}}{\partial \beta}\frac{\partial \beta}{\partial b_2} = -\frac{b_1}{b_2^2}\frac{\partial V_\mathrm{p}}{\partial \beta}, \tag{35}$$

$$\frac{\partial V_\mathrm{p}}{\partial h} = \frac{1}{\varepsilon_0\varepsilon_\mathrm{r}Q(\eta_\mathrm{p}, \alpha)V_\mathrm{p}}\frac{\partial K}{\partial h}, \tag{36}$$

$$\frac{\partial V_\mathrm{p}}{\partial g_0} = \frac{1}{\varepsilon_0\varepsilon_\mathrm{r}Q(\eta_\mathrm{p}, \alpha)V_\mathrm{p}}\frac{\partial K}{\partial g_0}. \tag{37}$$

From Eq. (10), the partial derivative of K with respect to the structural parameters can be obtained by

$$\frac{\partial K}{\partial L_1} = -\frac{1}{12}\kappa E h^3 g_0^3 \Big(\frac{4}{L^5}(2\beta\zeta_1 + \zeta_2) - \frac{L_2}{L^6}\Big(2\beta\frac{\partial \zeta_1}{\partial \alpha} + \frac{\partial \zeta_2}{\partial \alpha}\Big)\Big), \tag{38}$$

$$\frac{\partial K}{\partial L_2} = -\frac{1}{12}\kappa E h^3 g_0^3 \Big(\frac{4}{L^5}(2\beta\zeta_1 + \zeta_2) + \frac{L_1}{L^6}\Big(2\beta\frac{\partial \zeta_1}{\partial \alpha} + \frac{\partial \zeta_2}{\partial \alpha}\Big)\Big), \tag{39}$$

$$\frac{\partial K}{\partial h} = \frac{1}{L^4} g_0^3 \Big(\frac{1}{4}E h^2 + \mu l^2\Big)(2\beta\zeta_1 + \zeta_2), \tag{40}$$

$$\frac{\partial K}{\partial g_0} = \frac{1}{4L^4}\kappa E h^3 g_0^2 (2\beta\zeta_1 + \zeta_2). \tag{41}$$

The partial derivative of $Q(\eta_{\mathrm{p}}, \alpha)$ with respect to the structural parameters can be obtained by

$$\frac{\partial Q(\eta_{\mathrm{p}}, \alpha)}{\partial L_1} = \frac{\partial Q(\eta_{\mathrm{p}}, \alpha)}{\partial \alpha}\frac{\partial \alpha}{\partial L_1} = \frac{L_2}{L^2}\frac{\partial Q(\eta_{\mathrm{p}}, \alpha)}{\partial \alpha}, \tag{42}$$

$$\frac{\partial Q(\eta_{\mathrm{p}}, \alpha)}{\partial L_2} = \frac{\partial Q(\eta_{\mathrm{p}}, \alpha)}{\partial \alpha}\frac{\partial \alpha}{\partial L_2} = -\frac{L_1}{L^2}\frac{\partial Q(\eta_{\mathrm{p}}, \alpha)}{\partial \alpha}. \tag{43}$$

It is pointed out that the coefficient η_{p} in Eqs. (22), (32), and (33) must be recalculated for each new value of α, L_1, and L_2, respectively, due to its dependence on these parameters. From Eqs. (20)–(23) and (32)–(37), we can see that the sensitivities of the pull-in voltage to the material, dimensionless, and geometrical parameters depend on these parameters themselves.

3 Numerical simulation

3.1 Solution validation

The validity of the present model is verified through the comparison between the approximate analytical results and the numerical solutions based on the commercial ANSYS software. Consider the RF MEMS switch made of Au subjected to a bias V (see Fig. 2).

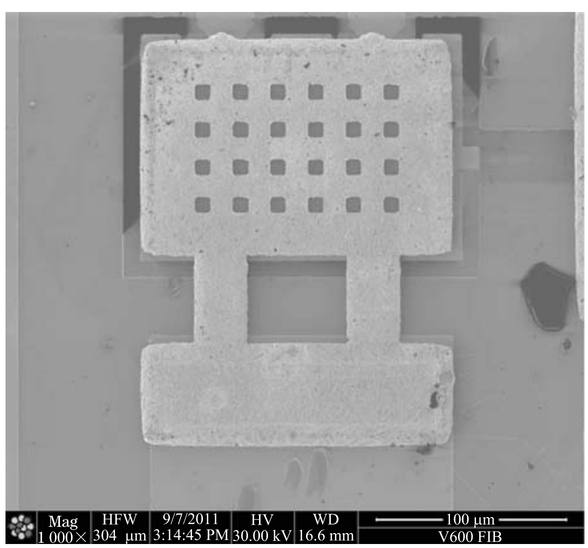

Fig. 2 Focused ion beam (FIB) image of RF MEMS switch: mag, magnification; HFW, horizontal field width; HV, high voltage; WD, work distance

The structural and material parameters are as follows:

$$\begin{cases} E = 78.5\,\text{GPa}, \quad \nu = 0.22, \quad l = 0, \\ b_1 = 34\,\mu\text{m}, \quad b_2 = 164\,\mu\text{m}, \quad L_1 = 46\,\mu\text{m}, \\ L_2 = 94\,\mu\text{m}, \quad h = 7\,\mu\text{m}, \quad g_0 = 2\,\mu\text{m}, \\ \varepsilon_0 = 8.854 \times 10^{-12}\,\text{F} \cdot \text{m}^{-1}, \quad \varepsilon_\text{r} = 1, \end{cases}$$

where E is the Young modulus, ν is the Possion ratio, l is the material length scale parameter, b_1 is the cantilever bar width, b_2 is the beam width, L_1 is the cantilever bar length, L_2 is the beam length, h is the beam thickness, g_0 is the initial gap height, ε_0 is the permittivity of the free space, and ε_r is the dielectric constant.

For a constant bias input, the deflections at the tip of the cantilever beam are calculated based on Eqs. (4) and (16).

Figure 3 shows the gap height at the cantilever tip calculated from the present model and the commercial ANSYS software. It can be seen that the analytical solutions obtained by the present model are apparently very close to the finite element solutions since the applied voltages are less than the pull-in voltage. The predicted pull-in voltage based on the present model is 97.6 V, and is close to the result of 91.2 V obtained from the ANSYS. The error percentage is only 7%. Therefore, the validity and accuracy of the present model is verified.

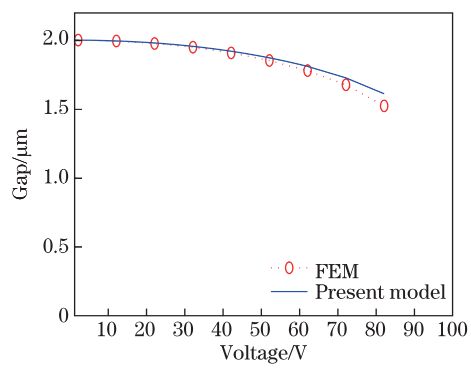

Fig. 3 Gap height between cantilever tip and substrate against applied voltage

3.2 Sensitivity analysis of pull-in voltage

In this section, the sensitivities of the pull-in voltage to the material, dimensionless, and structural parameters are investigated. It is noted that the high sensitivity of the pull-in voltage implying parameter perturbation can induce large changes in the pull-in voltage, which can affect the reliability of the MEMS devices. Therefore, for a perfect or optimal design, the pull-in voltage sensitivities to the designing parameters must be as low as possible.

Figure 4 plots the sensitivity functions of the pull-in voltage to the material parameters, where "design point" corresponds to the sensitivity value in the case study. The positive sensitivity values indicate that the pull-in voltage increases when the parameters increase. It can be seen from Fig. 4(a) that the higher the material modulus is, the smaller the pull-in voltage sensitivity is, and the higher the pull-in voltage is. Compared with the material Au used in the case study, polysilicon, which is chosen as the switch material, leads to a lower sensitivity of the pull-in voltage due to its larger material modulus. However, this may induce a higher pull-in voltage. Therefore, the material must be chosen as carefully as possible. Figure 4(b) shows that the sensitivity of the pull-in voltage increases with the increase in the ratio of the material length scale parameter to the beam thickness. When the beam thickness comes close to the material length scale parameter, the sensitivity value exceeds 28, which means that the size effect becomes non-negligible.

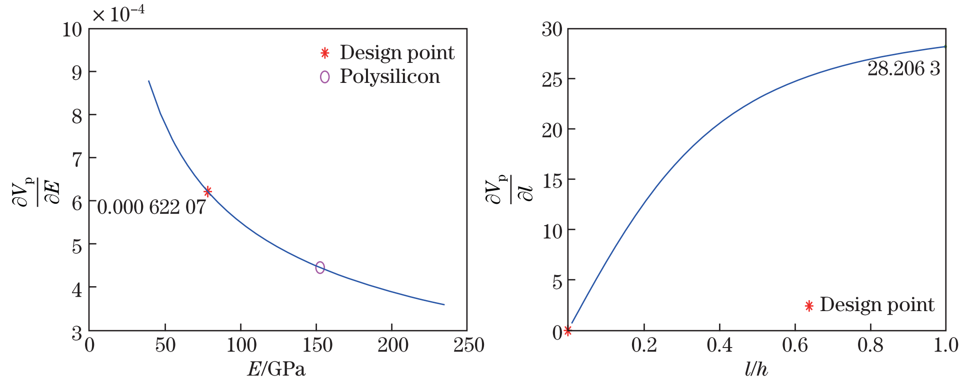

(a) Sensitivity to Young's modulus (b) Sensitivity to material length scale parameter

Fig. 4 Sensitivity functions of pull-in voltage to material parameters

Figure 5 is the sensitivity functions of the pull-in voltage to the dimensionless length ratio, where "design point" corresponds to the sensitivity value in the case study. It can be seen that, with the increase in the dimensionless parameter α, the sensitivity increases nonlinearly from negative to positive, which means that there exists a critical value where the corresponding pull-in sensitivity value is zero, e.g., the critical value is 0.494 4 in the case study, and the pull-in voltage is insensitive to the dimensionless length ratio α. It should be noted that the negative sensitivity values indicate the decreases in the pull-in voltage when the parameter increases. When the dimensionless length ratio α is less than the critical value, the pull-in voltage and its sensitivity to α decrease with the increase in the parameter α. When the dimensionless length ratio α is greater than the critical value, the pull-in voltage and its sensitivity to α increase with the increase in the parameter α. Therefore, the preferred dimensionless length ratio α must be close to but smaller than the critical value as soon as possible in order to obtain the lower pull-in voltage.

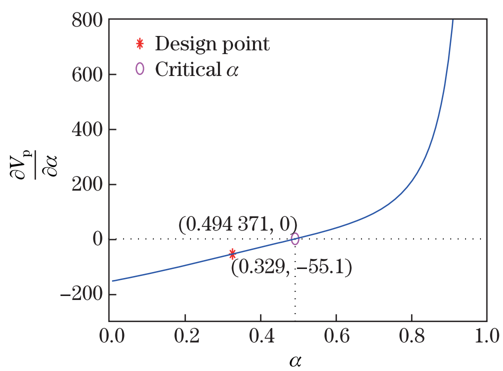

Fig. 5 Sensitivity function of pull-in voltage to dimensionless length ratio

In order to get a more general conclusion, let

$$\frac{\partial V_{\mathrm{p}}}{\partial \alpha} = 0.$$

Then, substituting Eqs. (24) and (31) into Eq. (22) leads to

$$\Big(2\beta\frac{\partial\zeta_1}{\partial\alpha}+\frac{\partial\zeta_2}{\partial\alpha}\Big)P(\eta_{\rm p},\alpha)+(2\beta\zeta_1+\zeta_2)F_1(\eta_{\rm p},\alpha)=0. \tag{44}$$

From Eqs. (18) and (44), it can be seen that the dimensionless parameter α is a function of the dimensionless width ratio β only. For a given β, the critical value of the dimensionless length ratio α has a unique solution. When $\beta=0.5$, corresponding to a constant cross-section beam, by substituting Eq. (26) into Eq. (44), we can simplify the equation as follows:

$$(\zeta_1+\zeta_2)F_1(\eta_{\rm p},\alpha)=0. \tag{45}$$

The natural mode satisfies the following equation[18]:

$$\int_0^1 \varphi''^2(X)\mathrm{d}X=\lambda^4. \tag{46}$$

Substituting Eqs. (13), (14), and (46) into Eq. (45) yields

$$\lambda^4\frac{\varphi(\alpha)}{(1-\eta_{\rm p}\varphi(\alpha))^2}=0. \tag{47}$$

The equivalent form of Eq. (47) is

$$\varphi(\alpha)=0. \tag{48}$$

Since the natural mode satisfies the boundary condition of the cantilever beam, Eq. (48) has a unique solution, i.e., $\alpha=0$, which means that the derivative to α, called the sensitivity function, is always larger than or equal to zero for the constant cross-section beam, and the pull-in voltage increases with the increase in the parameter α.

In order to investigate the relationship among

$$\frac{\partial V_{\rm p}}{\partial L_1},\quad \frac{\partial V_{\rm p}}{\partial L_2},\quad \frac{\partial V_{\rm p}}{\partial\alpha},$$

substituting Eqs. (22), (38), (39), (42), and (43) into Eqs. (32) and (33) and subtracting Eq. (32) from Eq. (33) yield

$$\frac{\partial V_{\rm p}}{\partial L_1}-\frac{\partial V_{\rm p}}{\partial L_2}=\frac{1}{L}\frac{\partial V_{\rm p}}{\partial\alpha}. \tag{49}$$

Therefore, when

$$\frac{\partial V_{\rm p}}{\partial\alpha}=0,$$

the pull-in voltage sensitivities to the beam length L_1 and the fixed electrode length L_2 are equal to each other. In order to explain the effect on the reduction of the pull-in voltage, the objective function is defined by

$$f(\alpha)=\Big(\frac{\partial V_{\rm p}}{\partial L_1}\Big)^2+\Big(\frac{\partial V_{\rm p}}{\partial L_2}\Big)^2. \tag{50}$$

As we all know, when

$$\Big|\frac{\partial V_{\rm p}}{\partial L_1}\Big|=\Big|\frac{\partial V_{\rm p}}{\partial L_2}\Big|,$$

the objective function $f(\alpha)$ can be minimized, and the minimum value is

$$2\left|\frac{\partial V_{\mathrm{p}}}{\partial L_1}\right| \times \left|\frac{\partial V_{\mathrm{p}}}{\partial L_2}\right|.$$

Therefore, the equation $\frac{\partial V_{\mathrm{p}}}{\partial \alpha} = 0$ is a necessary condition for minimizing $\frac{\partial V_{\mathrm{p}}}{\partial L_1}$ and $\frac{\partial V_{\mathrm{p}}}{\partial L_2}$ simultaneously.

Figure 6 plots the critical values of the dimensionless length ratio α against the dimensionless width ratio β, where "design point" corresponds to the sensitivity value in the studied case. From the figure, we can see that when β increases, the critical value of α decreases accordingly. For a given β, the optimal design point should fall on the curve of the figure.

Figure 7 shows the sensitivity function of the pull-in voltage to the dimensionless width ratio β, where "design point" corresponds to the sensitivity value in the case study. It can be seen that, when the dimensionless parameter β increases, the corresponding sensitivity decreases monotonically. When the parameter is 0.5, which denotes a constant cross-section beam, the pull-in voltage sensitivity can be minimized, while the pull-in voltage increases due to the positive sensitivity values.

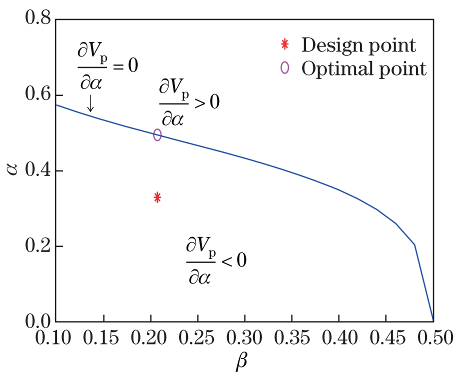

Fig. 6 Dimensionless length ratio against dimensionless width ratio

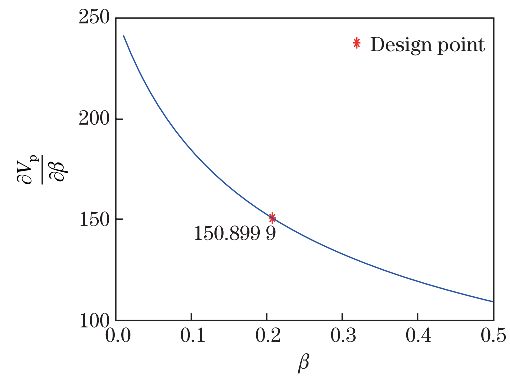

Fig. 7 Sensitivity function of pull-in voltage to dimensionless width ratio

Figure 8 plots the sensitivity functions of the pull-in voltage to the structural parameters. It can be seen that the pull-in voltage sensitivities are nonlinear functions of these structural parameters, respectively, increasing with the increases in the beam thickness h and the gap height g_0 while decreasing with the increases in the beam widths b_1 and b_2 and the beam lengths L_1 and L_2. However, the pull-in voltage increases with the increases in the beam width b_1, the beam thickness h, and the gap height g_0, while decreases with the increases in the beam width b_2 and the beam lengths L_1 and L_2. Since all the structural parameters have the same dimension, the modified parameters can be chosen directly in order to obtain the lower pull-in voltage efficiently by comparing the sensitivity values. The beam thickness h and the gap height g_0 can be chosen as the preferred modified parameters in the case study due to the higher sensitivity values.

Table 2 lists the relationship among the pull-in voltage, the sensitivity, and the parameters, where the upward arrow "↑" and the downward arrow "↓" denote increase and decrease, respectively. It can be seen that the pull-in voltage and the corresponding sensitivity decrease simultaneously with the increases in the beam width b_2 and the beam lengths L_1 and L_2, while increase with the increases in the beam thickness h and the gap height g_0. Moreover, the increase in the beam width b_1 leads to the increase in the pull-in voltage and the decrease in the corresponding sensitivity.

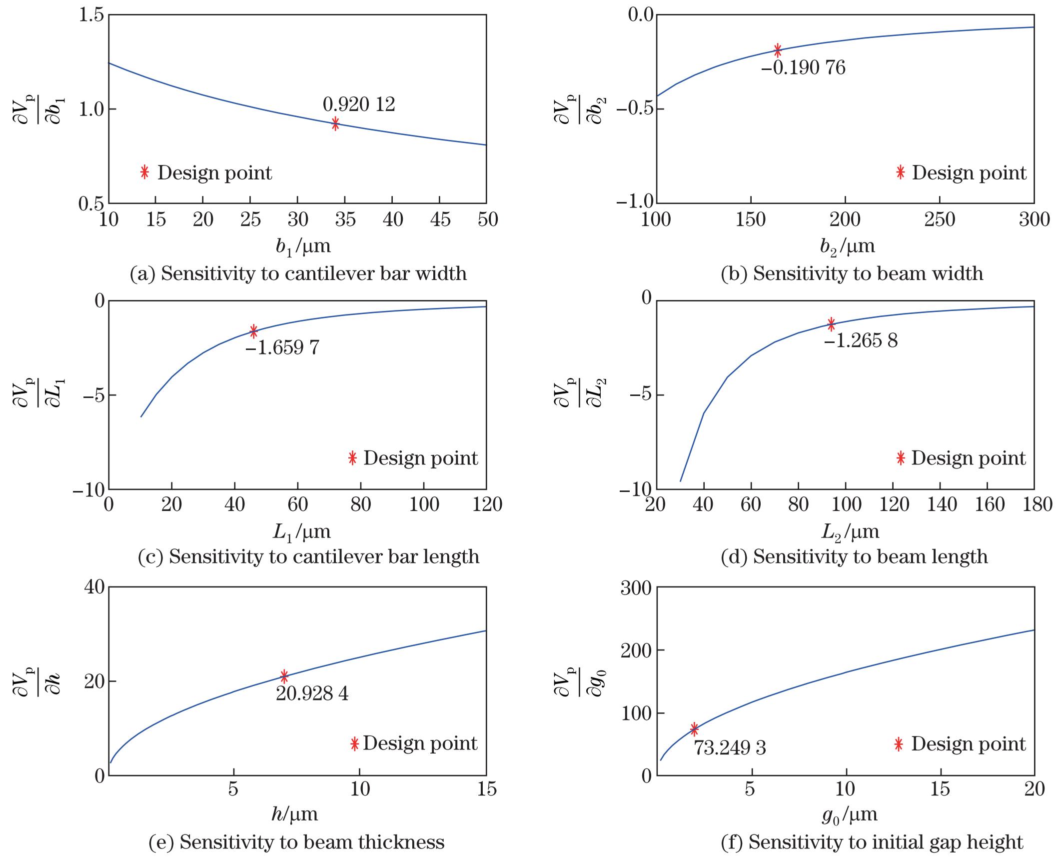

Fig. 8 Sensitivity functions of pull-in voltage to structural parameters

Table 1 List of relationship among pull-in voltage, sensitivity, and parameters

Parameters (X)	Pull-in voltage (V_p)	Corresponding sensitivity ($\mathrm{d}V_\mathrm{p}/\mathrm{d}X$)
Young's modulus (E)	↑	↓
Material length scale parameter (l)	↑	↑
Dimensionless length ratio (α)	First ↓ and then ↑	First ↓ and then ↑
Dimensionless width ratio (β)	↑	↓
Cantilever bar width (b_1)	↑	↓
Beam width (b_2)	↓	↓
Cantilever bar length (L_1)	↓	↓
Beam length (L_2)	↓	↓
Beam thickness (h)	↑	↑
Initial gap height (g_0)	↑	↑

4 Summary

In this paper, an approximate analytical solution for the pull-in voltage of a stepped cantilever-type RF MEMS switch is presented based on the Euler-Bernoulli beam theory and a modified couple stress theory to investigate the sensitivities of the pull-in voltage to various parameters, e.g., the material parameters, the dimensionless parameters, and the structural parameters. The correctness and high accuracy of the present model are verified by comparison with the finite element solutions. Moreover, the sensitivity functions of the pull-in voltage to various parameters are derived explicitly. Some new merits of the stepped cantilever beam are observed. The main contributions of this study are listed as follows:

(i) The modeling method for the stepped cantilever-type structure is correct and effective. The prediction model includes the size effect, and can be used to predict the pull-in voltage of the similar structure in the micro/nano scale.

(ii) The sensitivities of the pull-in voltage to the material parameters vary nonlinearly with the material parameters. Large material modulus can reduce the sensitivity of the pull-in voltage and increase the pull-in voltage. When the beam thickness comes close to the material length scale parameter, the sensitivity to the material length scale parameter becomes larger, and the size effect becomes non-negligible.

(iii) There exists a unique optimal dimensionless length ratio, where the pull-in voltage is insensitive. The critical value only depends on the dimensionless width ratio. For a constant cross-section cantilever beam, the critical value is zero, the sensitivity to the dimensionless length ratio is always greater than or equal to zero, and the dimensionless length ratio corresponding to the minimum pull-in voltage is zero. In order to obtain lower pull-in voltages, the optimal dimensionless length ratio α must be close to but less than the critical value. The decrease in the pull-in voltage results in the decrease in the corresponding sensitivity to the dimensionless width ratio β inevitably.

(iv) The pull-in voltage and the corresponding sensitivity decrease simultaneously with the increases in the beam width b_2 and the beam lengths L_1 and L_2, and increase simultaneously with the increases in the beam thickness h and the gap height g_0. In order to reduce the pull-in voltage, these parameters must be chosen as the modified parameters first, while other parameters need to be designed as carefully as possible.

References

[1] Zhang, W. M., Yan, H., Peng, Z. K., and Meng, G. Electrostatic pull-in instability in MEMS/NEMS: a review. *Sensors and Actuators, A: Physical*, **214**, 187–218 (2014)

[2] Nathanson, H. C., Newell, W. E., Wickstrom, R. A., and Davis, J. R., Jr. The resonant gate transistor. *IEEE Transactions on Electron Devices*, **14**, 117–133 (1967)

[3] Osterberg, P. M. *Electrostatically Actuated Microelectromechanical Test Structures for Material Property Measurement*, Ph. D. dissertation, Massachusetts Institute of Technology, Massachusetts (1995)

[4] Rokni, H., Seethaler, R. J., Milani, A. S., Hosseini-Hashemi, S., and Li, X. F. Analytical closed-form solutions for size-dependent static pull-in behavior in electrostatic micro-actuators via Fredholm integral equation. *Sensors and Actuators, A: Physical*, **190**, 32–43 (2013)

[5] Noghrehabadi, A., Eslami, M., and Ghalambaz, M. Influence of size effect and elastic boundary condition on the pull-in instability of nano-scale cantilever beams immersed in liquid electrolytes. *International Journal of Non-Linear Mechanics*, **52**, 73–84 (2013)

[6] Baghani, M. Analytical study on size-dependent static pull-in voltage of microcantilevers using the modified couple stress theory. *International Journal of Engineering Science*, **54**, 99–105 (2012)

[7] Raeisifard, H., Bahrami, M. N., Yousefi-Koma, A., and Fard, R. H. Static characterization and pull-in voltage of a micro-switch under both electrostatic and piezoelectric excitations. *European Journal of Mechanics, A: Solids*, **44**, 116–124 (2014)

[8] Huang, Y. T., Chen, H. L., and Hsu, W. An analytical model for calculating the pull-in voltage of micro cantilever beams subjected to tilted and curled effects. *Microelectronic Engineering*, **125**, 73–77 (2014)

[9] Zhang, J. and Fu, Y. Pull-in analysis of electrically actuated viscoelastic microbeams based on a modified couple stress theory. *Meccanica*, **47**, 1649–1658 (2012)

[10] Wang, B., Zhou, S., Zhao, J., and Chen, X. Size-dependent pull-in instability of electrostatically actuated microbeam-based MEMS. *Journal of Micromechanics and Microengineering*, **21**, 027001 (2011)

[11] Yang, J., Jia, X., and Kitipornchai, S. Pull-in instability of nano-switches using nonlocal elasticity theory. *Journal of Physics*, *D*: *Applied Physics*, **41**, 035103 (2008)

[12] Schrag, G., Kunzig, T., and Wachutka, G. Modeling reliablity issues in RF MEMS switches. *International Conference on Simulation of Semiconductor Processes and Devices* (*SISPAD*), Glasgow, 432–435 (2013)

[13] Rebeiz, G. M. *RF MEMS Theory*, *Design*, *and Technology*, John Wiley and Sons, New York (2003)

[14] Kong, S. Size effect on pull-in behavior of electrostatically actuated microbeams based on a modified couple stress theory. *Applied Mathematical Modelling*, **37**, 7481–7488 (2013)

[15] Zhang, Y. and Zhao, Y. P. Numerical and analytical study on the pull-in instability of micro-structure under electrostatic loading. *Sensors and Actuators*, *A*: *Physical*, **127**, 366–380 (2006)

[16] Hu, Y. C. Closed form solutions for the pull-in voltage of micro curled beams subjected to electrostatic loads. *Journal of Micromechanics and Microengineering*, **16**, 648–655 (2006)

[17] Spiegel, M. R., Lipschutz, S., and Liu, J. *Mathematical Handbook of Formulas and Tables*, McGraw-Hill, New York (2009)

[18] Hu, Y. C., Chang, C. M., and Huang, S. C. Some design considerations on the electrostatically actuated microstructures. *Sensors and Actuators*, *A*: *Physical*, **112**, 155–161 (2004)